SAND95-2635C
CONF-960738--1

APPLICATION OF GAMMA-DENSITOMETRY TOMOGRAPHY TO DETERMINE PHASE SPATIAL VARIATION IN TWO-PHASE AND THREE-PHASE BUBBLY FLOWS*

J. R. Torczynski, D. R. Adkins, K. A. Shollenberger, and T. J. O'Hern
Engineering Sciences Center
Sandia National Laboratories
Albuquerque, New Mexico 87185-5800

ABSTRACT

Gamma-densitometry tomography is applied to two-phase and three-phase bubbly flows. Spatially resolved measurements of the phase volume fractions are presented for air-water and air-water-sand experiments at various airflow rates. For the conditions examined, the presence of the solid particulate phase had only a minimal effect on the gas volume fraction spatial variation.

NOMENCLATURE

c_{mn}	=	inverse Abel transform coefficient (nondimensional)
d_{mn}	=	forward Abel transform coefficients (nondimensional)
g	=	gravitational acceleration (cm/s^2)
H	=	height of air-water interface during airflow (cm)
H_0	=	height of air-water interface without airflow (cm)
I	=	intensity (photon/s)
I_0	=	incident intensity (photon/s)
i	=	data point index (positive integer)
L	=	path length through attenuating material (cm)
m, n	=	matrix indices (nonnegative integers)
p	=	pressure (dyne/cm^2)
r	=	radial position (cm)
x	=	horizontal position (cm)
z	=	vertical position (cm)
μ	=	attenuation coefficient (cm^{-1})
μ/ρ	=	mass attenuation coefficient (cm^2/g)
ρ	=	mass density (g/cm^3)
ψ	=	normalized attenuation coefficient (nondimensional)
$\tilde{}$	=	average value along path L

*This work was performed at Sandia National Laboratories, supported by the U. S. Department of Energy, under contract number DE-AC04-94AL85000.

INTRODUCTION

Knowledge of the spatial variations of phase volume fractions in two-phase and three-phase flows is important in many industrial processes such as indirect coal liquefaction, in which a reactive gas is bubbled through a catalyst-laden liquid (a slurry). More specifically, process efficiency can be affected adversely by significant spatial nonuniformity in gas volume fraction, which can induce large-scale buoyancy-driven recirculating flows. Thus, it is important to be able to characterize the phase volume fraction spatial variation in multiphase flows.

One method of characterizing the phase volume spatial variation is gamma-densitometry tomography (GDT). The basic physics of the interaction of gamma photons with matter is well known (cf. Meyerhof (1967) or Lamarsh (1983)). In brief, there are three interaction mechanisms: the photoelectric effect, pair production, and Compton scattering. The first two are absorptive (the gamma photon disappears), whereas the last one is not (the energy and direction of the gamma photon change). These processes cumulatively yield a mass attenuation coefficient μ/ρ (units of cm^2/g), a constant depending only on the composition of the material and the gamma photon energy. When multiplied by the mass density ρ, here assumed to be constant, the attenuation coefficient μ describes the attenuation of a gamma beam of intensity I passing along a path of length L through the material: $I = I_0 \exp(-\mu L)$. If a mixture of two materials with different μ values is present along the path, a measurement of I/I_0 yields the average attenuation coefficient $\tilde{\mu}$ along the path L, where the value of μ at each point along the path is linearly related to the material volume fractions comprising the mixture at that point. Measuring $\tilde{\mu}$ in this manner along many different paths provides the information needed to perform a tomographic reconstruction of the spatial variation of μ and hence the volume fraction spatial distribution of the materials comprising the mixture. The varieties of tomographic reconstruction algorithms which accomplish this

are discussed in great detail elsewhere (e.g. entire issues of the IEEE Proceedings, as summarized by Herman (1983), and of Applied Optics, edited by Howard (1985)). A description of the Abel transform for axisymmetric spatial variation can be found in Vest (1985).

Investigators have long recognized the potential of GDT to probe multiphase flows. Typical applications have included two-phase gas-liquid pipe flows for the nuclear industry (Hewitt, 1978), saturation measurements in porous media (Reda et al., 1981), gas-solid fluidized beds (MacCuaig et al., 1985), bubble columns (Kumar et al., 1995), and horizontal stratified three-phase pipe flow (Pan and Hewitt, 1995). In the present study, GDT is applied to determine the phase spatial variations in two-phase air-water flow and three-phase air-water-particulate flow.

EXPERIMENT AND ANALYSIS

The GDT system in this study uses a 5-Curie Cs-137 isotope source to provide a beam of 0.6616 MeV gamma photons. The source is contained in a cylindrical lead vault with a small-diameter aperture to produce a collimated beam. The individual gamma photons are observed with a sodium iodide (NaI) scintillation detector, the temperature of which is controlled to minimize thermally induced drift. To avoid spurious acquisition of gamma photons that have been scattered through small angles, a small-diameter aperture is placed in front of the detector to provide angular selectivity. Additionally, a multichannel analyzer is used to select lower and upper energy cutoffs so that only the gamma photons lying within this energy "window" are counted: scattered photons, which have lower energy, are screened out. The source and the detector are mounted on two opposing arms of a heavy-duty computer-controlled two-axis traverse. This traverse has 60 cm of travel in both the horizontal and the vertical directions, and the arms have 66 cm of clearance to accommodate large testbeds. Operation of this system is fully automated: a user selects a scan direction (vertical or horizontal), a step size (distance from one path to the next), and either a time to collect data for each path during which counts are recorded or a minimum number of counts where the time to observe them is recorded.

The flow system under examination is a bubble column fabricated out of a lucite tube with outer and inner diameters of 20.3 cm and 19.0 cm, respectively, and a height of 1.8 m (see Figure 1). To preclude overflow, the column is filled to an initial height of 1.2 m, a height-to-diameter ratio of about 6. In this study, the working fluids are air and water, and operation is at ambient temperature and pressure. Gas is introduced near the bottom of the column via a sparger, a 9 cm diameter ring spiral made from 0.25" OD copper tubing in which 12 downward-facing holes of 0.08" diameter have been drilled at equal azimuthal intervals. As currently configured, airflow rates of up to 600 lpm are routinely achievable, which corresponds to gas superficial velocities up to roughly 35 cm/s. It is also possible to introduce a third phase of solid particulates into the column, such as sand or glass spheres.

Due to the time required to obtain sufficient counts, all GDT results for this flow system are inherently time-averaged. A small systematic error is thus introduced since the time-averaged intensity does not correspond exactly to the time-averaged attenuation coefficient. However, errors appear to be small for these flows based on comparison to level-rise measurements.

GDT data are acquired and analyzed in the following manner. The time-averaged flow is taken to be axisymmetric, which appears to be a reasonable assumption based on the fact that data from the left and right halves of the column are roughly mirror images of each other. Given the assumption of axisymmetry, only one "projection" of data is required: the intensities I_i are measured at a series of horizontal positions x_i while the vertical position z is held constant. To acquire the data needed to reconstruct the phase volume fraction spatial variations, this type of scan is performed for three different conditions: first, with the column "empty" (i.e. full of air only); second, with the column "full" (i.e. full of water); third, with the actual multiphase flow. If multiple flow rates are desired, the same "full" and "empty" scans can be used. These data then yield values for the path-averaged normalized attenuation coefficient $\tilde{\psi}_i$ at each position x_i:

$$\tilde{\psi}_i = \frac{\tilde{\mu}_i^{\text{flow}} - \tilde{\mu}_i^{\text{empty}}}{\tilde{\mu}_i^{\text{full}} - \tilde{\mu}_i^{\text{empty}}} = \frac{\ln\left(I_i^{\text{empty}}\right) - \ln\left(I_i^{\text{flow}}\right)}{\ln\left(I_i^{\text{empty}}\right) - \ln\left(I_i^{\text{full}}\right)}$$

The Abel transform (cf. Vest (1985)) can be applied to the data set $\{(x_i, \tilde{\psi}_i)\}$ to determine the radial variation of ψ within a circular domain of radius R. For the representations

$$\psi(r,R) = \sum_{m=0}^{N} a_m (r/R)^{2m}, \quad \tilde{\psi}(x,R) = \sum_{n=0}^{N} b_n (x/R)^{2n}$$

the following reconstruction relations are obtained:

$$a_m = \sum_{n=0}^{N} c_{mn} b_n, \quad b_n = \sum_{m=0}^{N} d_{nm} a_m$$

where in terms of binomial coefficients

$$c_{mn} = \begin{cases} -\left[\dfrac{2m+1}{2^{2n}(2n-2m-1)}\right]\binom{2n-2m}{n-m}\binom{2m}{m}, & m \le n \\ 0, & m > n \end{cases}$$

$$d_{nm} = \begin{cases} \left[\dfrac{2^{2n}}{2m+1}\right]\binom{2m-2n}{m-n}\Big/\binom{2m}{m}, & n \le m \\ 0, & n > m \end{cases}$$

Tomographic reconstruction of an axisymmetric spatial distribution of ψ proceeds in the following manner.

1. Measure the path-averaged attenuations $\tilde{\psi}_i$ on a set of paths x_i.
2. Fit the $\{(x_i, \tilde{\psi}_i)\}$ with even powers of x_i/R to find the b_n.
3. Use the c_{mn} to find the a_m and the attenuation radial variation ψ.

Note that for a two-phase gas-liquid flow, ψ corresponds to the liquid volume fraction in the medium and hence is zero for pure gas and unity for pure liquid. In a three-phase flow, additional information is needed to relate ψ to the phase volume fractions.

Table 1: Average gas volume fraction for two-phase flow.

Air Flow (lpm)	Sup. Vel. (cm/s)	Level Rise	Pres. Diff.	GDT
100	5.9	0.11	0.11	0.12
200	11.8	0.17	0.17	0.19
300	17.7	0.22	0.20	0.24

RESULTS

Gas-liquid two-phase flow experiments have been performed using air and water in the bubble column described above. Horizontal GDT scans were taken at a height of 3 diameters above the bubble-column base, with data taken across the bubble column at 0.5 cm intervals. Scans are performed with the column full of water, empty, and with three airflow rates: 100, 200, and 300 lpm, which correspond to gas superficial velocities of 5.9, 11.8, and 17.7 cm/s, respectively. Figure 2 shows the spatial variation of the ratio of the attenuation coefficient of the mixture for the highest airflow rate examined. Results have been normalized by the attenuation coefficient of pure water for convenience. Here $\bar{\psi}$ and ψ denote "path-averaged" and "radial variation", respectively. Figure 3 shows the radial variations of the gas and liquid volume fractions for this case. The lower airflow cases (not shown) are qualitatively similar but have smaller gas volume fractions. In all cases examined, the gas volume fraction obtains its maximum value on axis and increases with increasing gas superficial velocity, as expected.

As a check, two other methods were used to yield information about the gas volume fraction. First, level-rise measurements were performed to determine the average gas volume fraction for the entire column. If H_0 is the original height of the air-water interface without airflow and H is the interface height with airflow, then the average gas volume fraction is given by $(H-H_0)/H$. Second, pressure-difference measurements were performed to determine the average gas volume fraction in a one-diameter length of the column centered about the GDT measurement plane. Since the pressure in the column is approximately hydrostatic, the average gas volume fraction is given by $[1+(dp/dz)/(\rho g)]$, where ρ is the liquid density, g the gravitational acceleration, and dp/dz the vertical pressure gradient (negative). The average gas volume fractions determined from GDT and the above two methods are shown in Table 1 and are seen to agree reasonably well.

Gas-liquid-solid three-phase flow experiments have also been performed using air, water, and sand (particle diameters 0.1-0.4 mm) in the bubble column described above. A horizontal GDT scan has been taken as above with an airflow rate of 300 lpm. Figure 4 shows the spatial variation in the normalized attenuation coefficient ratio for this case. Also, an additional scan has been made without airflow for the sediment at the bottom of the column, which is fairly densely packed sand completely infiltrated with water. GDT and the phase rule (phase volume fractions sum to unity) do not provide enough information to determine all three unknown volume-fraction spatial distributions (air, water, and sand). To achieve closure, an additional relation is required. One possible assumption is that all of the sand suspended in the flow (as differentiated from the sediment layer of sand at the bottom of the column) is distributed uniformly within the liquid phase: the solid and liquid volume fractions are proportional throughout the flow. Since the bubble-induced mixing appears strong, this assumption seems reasonable. Note, however, that this assumption constrains the radial variations of the liquid and solid volume fractions to be proportional. To determine the constant of proportionality, it is necessary to determine the amount of sand suspended during airflow. This was accomplished by measuring the height of the sediment layer that remained unsuspended during airflow and using the known volume fraction of sand in the sediment layer, previously measured to be 0.63. [The density and attenuation coefficient for sand were also measured and found to be 2.44 g/cm^3 and 0.2134 cm^{-1}, close to the values of 2.65 g/cm^3 and 0.2041 cm^{-1} for pure SiO_2 (cf. Weast (1973) and Lamarsh (1983)).] Prior to initiating airflow, 8.37 kg of sand, with an equivalent height of 19.1 cm, was added to the bubble column, which had previously been filled with water to a height of 76.2 cm. When an airflow of 300 lpm was initiated, the undisturbed sediment layer remaining on the bottom was found to be 7.6 cm thick, so the suspended water and sand (i.e. not in the sediment region) have effective heights of 73.4 cm and 7.2 cm, respectively. The ratio of these heights yields a value of 0.098 for the proportionality constant relating the sand volume fraction to the water volume fraction (valid only for this particular experiment). Figure 5 shows the radial variations of the gas, liquid, and solid volume fractions for this experiment, with average values of 0.231, 0.701, and 0.068, respectively. As in the two-phase flow experiments, the gas volume fraction is observed to obtain its maximum value on axis. Interestingly, the presence of the solid particulate phase had only a minimal effect on the air volume fraction, both in average value and in radial variation (compare Figures 3 and 5). No explanation is advanced at present for this observation, which should not be assumed to apply in general to other experimental conditions.

CONCLUSIONS AND FUTURE EFFORTS

Gamma-densitometry tomography has been successfully applied to make spatially resolved measurements of phase volume fractions in two-phase and three-phase bubbly flows. Future studies are focusing on performing more carefully controlled three-phase experiments over a wider range of flow rates and solids loadings. The solid particulate phase are 80 μm diameter glass beads, and pressure-difference measurements are being made simultaneously along with GDT to provide the additional information needed to determine all three volume fractions. This obviates the need for the reasonable but admittedly ad hoc assumption of uniform solids distribution in the liquid. Also, to examine conditions representative of industrial-scale slurry-phase bubble-column reactors, a stainless steel vessel 0.5 m in diameter and 2.75 m in height has been constructed that can operate using organic liquids and high catalyst mass loadings at elevated pressures and temperatures. Preliminary studies in this apparatus have verified that GDT can be applied to make gas volume fraction measurements.

ACKNOWLEDGMENTS

The authors are grateful for the excellent technical support provided by T. W. Grasser, J. J. O'Hare, and C. B. Lafferty of Sandia National Laboratories. This work was performed at Sandia National Laboratories, supported by the U. S. Department of Energy under contract number DE-AC04-94AL85000, through a laboratory directed research and development (LDRD) contract.

REFERENCES

Herman, G. T., 1983, "The Special Issue on Computerized Tomography," Proceedings of the IEEE, Vol. 71, No. 3, pp. 291-292.

Hewitt, G. F., 1978, *Measurement of Two-Phase Flow Parameters*, Academic Press, London.

Howard, J. N., ed., 1985, Applied Optics, Vol. 24, No. 23.

Kumar, S. B., Moslemian, D., Dudukovic, M. P., 1995, "A γ-Ray Tomographic Scanner for Imaging Voidage Distribution in Two-Phase Flow Systems," Flow Measurement and Instrumentation, Vol. 6, No. 1, pp. 61-73.

Lamarsh, J. R., 1983, *Introduction to Nuclear Engineering*, Addison-Wesley, Reading, MA, pp. 78-88, 472-488, 648-649.

MacCuaig, N., Seville, J. P. K., Gilboy, W. B., and Clift, R., 1985, "Application of Gamma-Ray Tomography to Gas Fluidized Beds," Applied Optics, Vol. 24, No. 23, pp. 4083-4085.

Meyerhof, W. E., 1967, *Elements of Nuclear Physics*, McGraw-Hill, New York, pp. 91-103.

Pan, L., and Hewitt, G. F., 1995, "Precise Measurement of Cross Sectional Phase Fractions in Three-Phase Flow Using a Dual-Energy Gamma Densitometer," ANS Proceedings, Thermal Hydraulics Division, Vol. 8, pp. 71-78.

Reda, D. C., Hadley, G. R., and Turner, J. R., 1981, "Application of the Gamma-Beam Attenuation Technique to the Measurement of Liquid Saturation for Two-Phase Flows in Porous Media," Instrumentation in the Aerospace Industry, Vol. 27, Advances in Test Measurement, Vol. 18, K. E. Kissell, ed., Instrument Society of America, Research Triangle Park, NC, pp. 553-568.

Vest, C. M., 1985, "Tomography for Properties of Materials that Bend Rays: A Tutorial," Applied Optics, Vol. 24, No. 23, pp. 4089-4094.

Weast, R. C., ed., 1973, *CRC Handbook of Chemistry and Physics*, 54th edition, CRC Press, Cleveland OH, p. B-133.

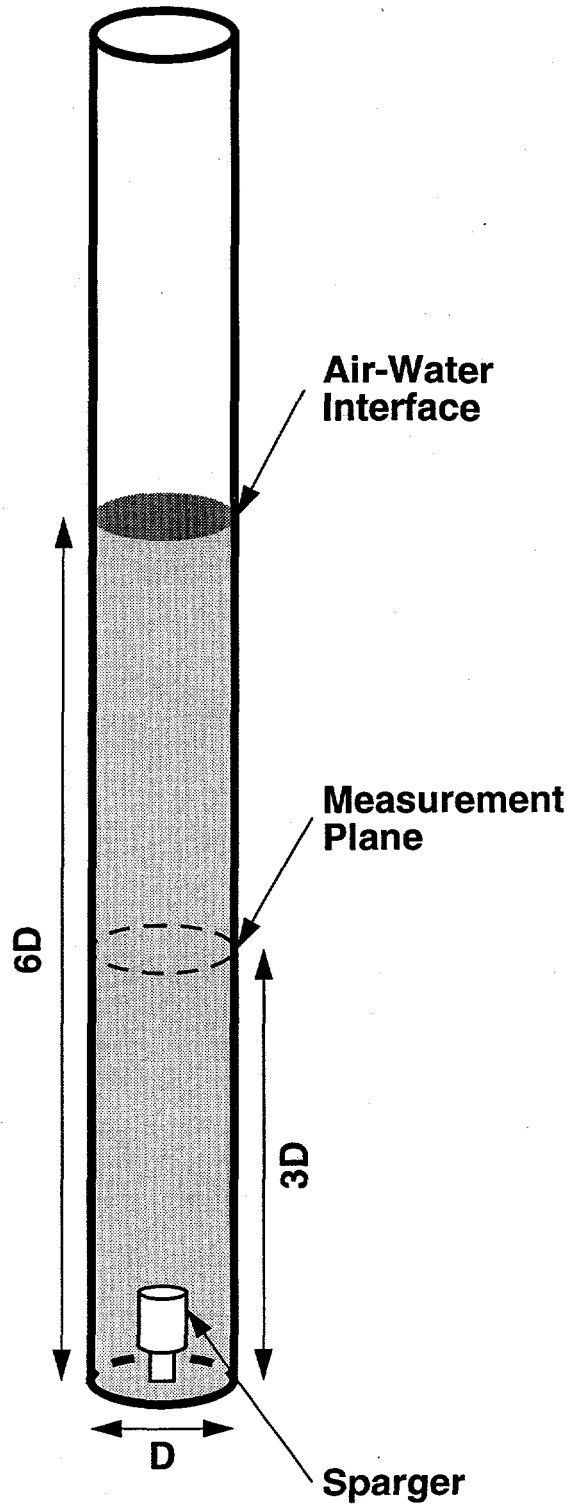

Figure 1. Schematic diagram of air-water bubble column.

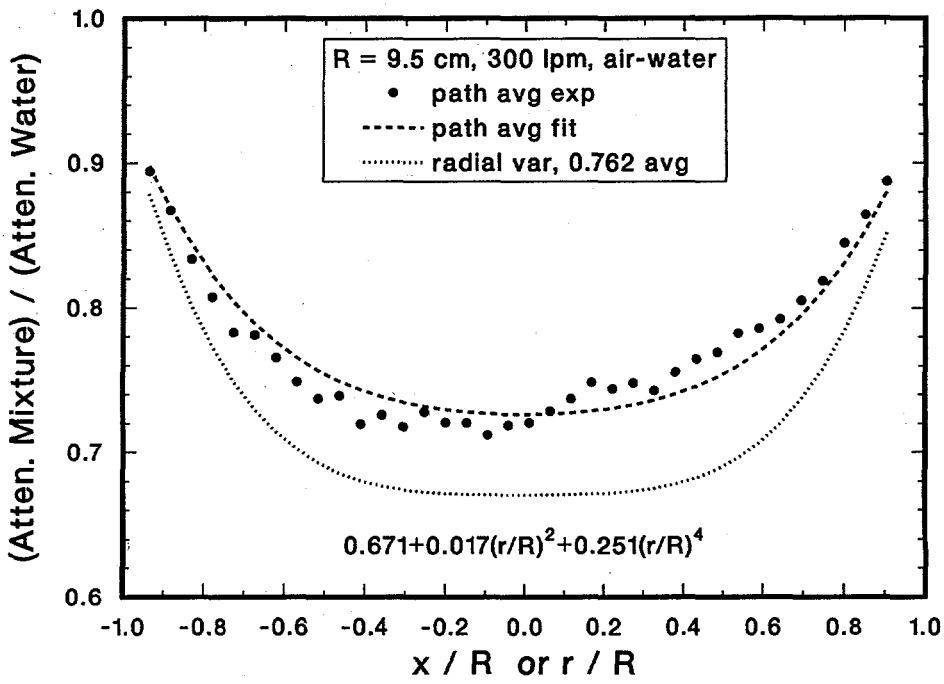

Figure 2. Spatial variation of normalized attenuation coefficient for air-water two-phase flow at 300 lpm. "Path-averaged" denotes the average normalized attenuation coefficient $\bar{\psi}$, and "radial variation" denotes its tomographically reconstructed radial variation ψ.

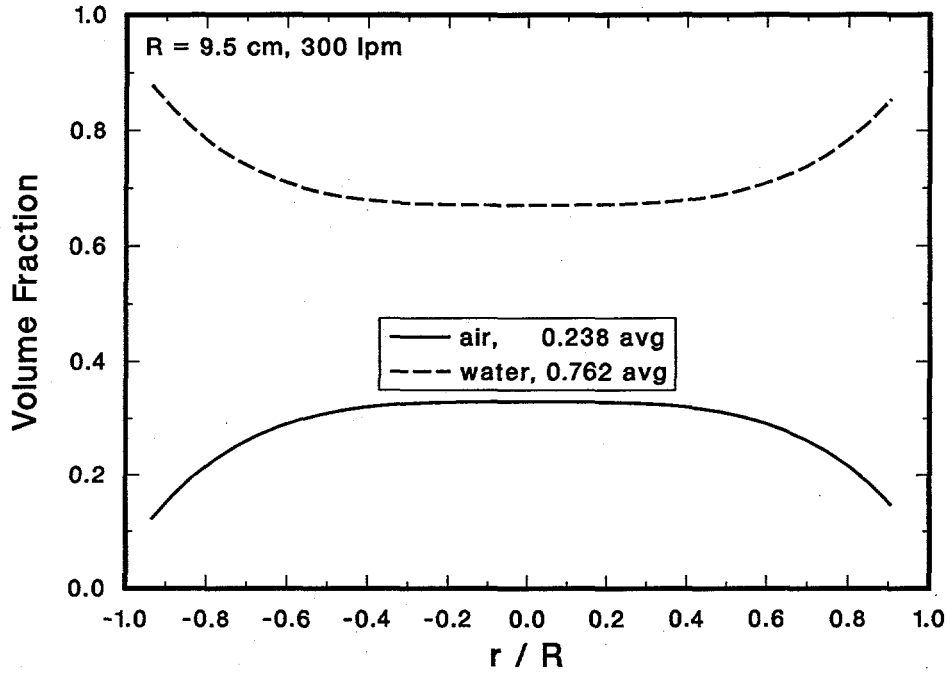

Figure 3. Radial variations of air and water volume fractions for air-water two-phase flow at 300 lpm. Averages are shown in the legend.

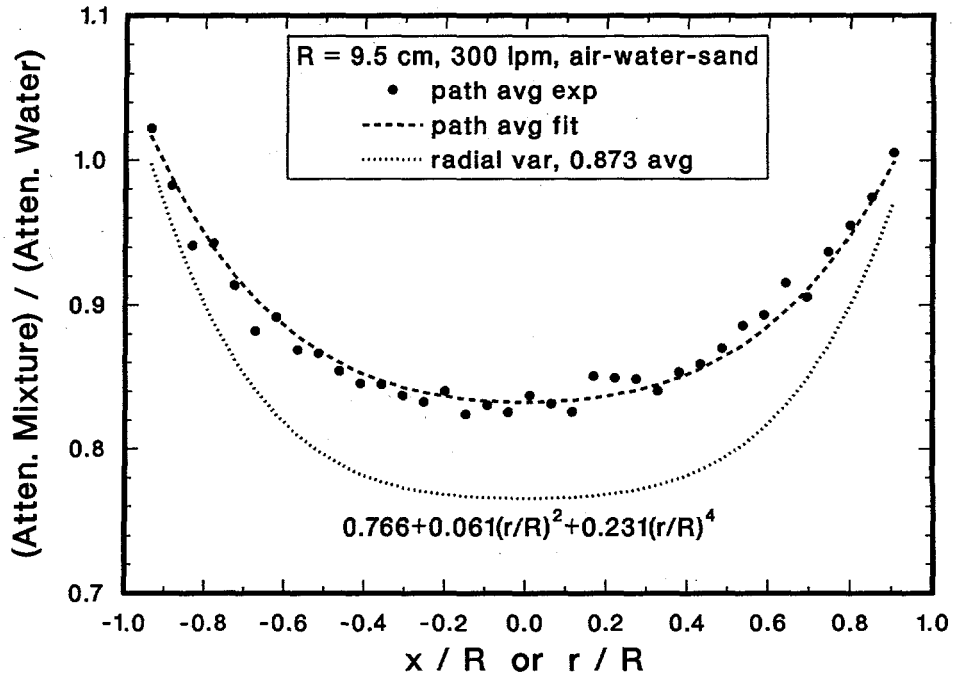

Figure 4. Spatial variation of normalized attenuation coefficient for air-water-sand three-phase flow at 300 lpm. "Path-averaged" denotes the average normalized attenuation coefficient $\tilde{\psi}$, and "radial variation" denotes its tomographically reconstructed radial variation ψ.

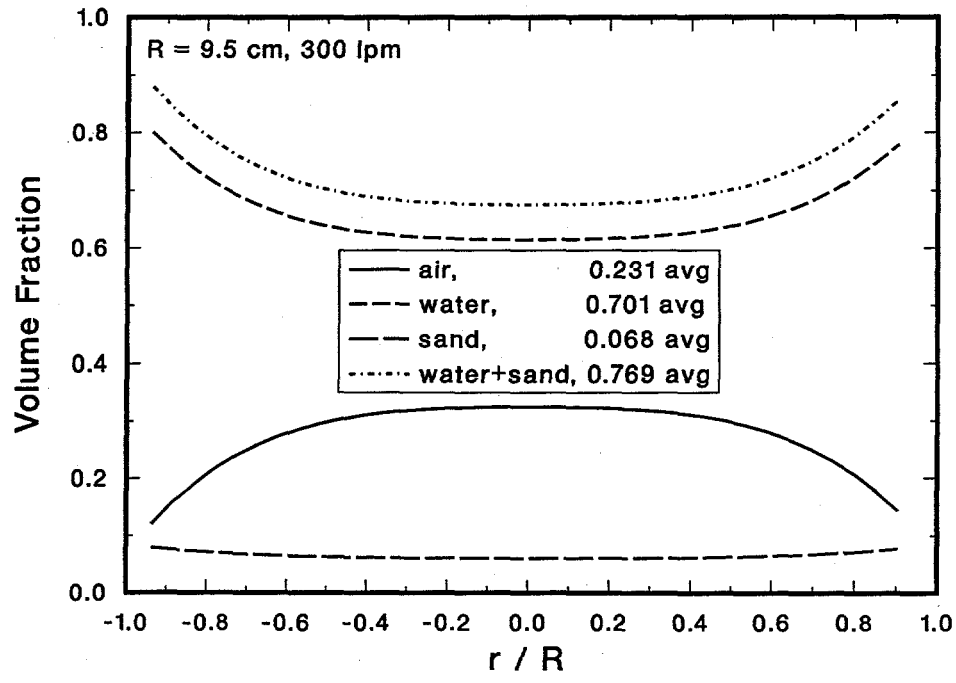

Figure 5. Radial variations of air, water, sand, and (water + sand) volume fractions for air-water-sand three-phase flow at 300 lpm. Averages are shown in the legend. The air volume fraction is almost identical to the two-phase result shown in Figure 3.